LETTER

doi:10.1038/nature12918

Localized sources of water vapour on the dwarf planet (1) Ceres

Michael Küppers[1], Laurence O'Rourke[1], Dominique Bockelée-Morvan[2], Vladimir Zakharov[2], Seungwon Lee[3], Paul von Allmen[3], Benoît Carry[1,4], David Teyssier[1], Anthony Marston[1], Thomas Müller[5], Jacques Crovisier[2], M. Antonietta Barucci[2] & Raphael Moreno[2]

The 'snowline' conventionally divides Solar System objects into dry bodies, ranging out to the main asteroid belt, and icy bodies beyond the belt. Models suggest that some of the icy bodies may have migrated into the asteroid belt[1]. Recent observations indicate the presence of water ice on the surface of some asteroids[2–4], with sublimation[5] a potential reason for the dust activity observed on others. Hydrated minerals have been found[6–8] on the surface of the largest object in the asteroid belt, the dwarf planet (1) Ceres, which is thought to be differentiated into a silicate core with an icy mantle[9–11]. The presence of water vapour around Ceres was suggested by a marginal detection of the photodissociation product of water, hydroxyl (ref. 12), but could not be confirmed by later, more sensitive observations[13]. Here we report the detection of water vapour around Ceres, with at least 10^{26} molecules being produced per second, originating from localized sources that seem to be linked to mid-latitude regions on the surface[14,15]. The water evaporation could be due to comet-like sublimation or to cryo-volcanism, in which volcanoes erupt volatiles such as water instead of molten rocks.

We observed Ceres with the Heterodyne Instrument for the Far Infrared (HIFI)[16] on the European Space Agency's Herschel Space Observatory[17] on four occasions between November 2011 and March 2013 (Extended Data Table 1) as part of the MACH-11 ('Measurements of 11 asteroids and comets with Herschel') guaranteed time programme (principal investigator L.O'R.) and of a follow-up Director's Discretionary Time Program. We used HIFI to search for water vapour directly, because it is more sensitive to water concentrated in the near-Ceres environment than previous instruments used to search for hydroxyl (OH). We observed the water ground-state line at a frequency of 556.936 GHz. The angular diameter of Ceres was <1 arcsec for all observations, compared to the beam width of HIFI, which was approximately 40 arcsec at the frequency of the water line. Although we cannot resolve Ceres spatially, we can derive information about the longitudinal distribution of the water sources on the surface from the variation of the absorption over the rotation of Ceres. Details of observations and data reduction are provided in the Supplementary Information and in Extended Data Table 1.

Figure 1 shows time-averaged spectra taken in October 2012 and on 6 March 2013, normalized to the thermal continuum of Ceres (measured with the expected brightness, see Extended Data Table 2). At the frequency of the water line, absorption in the thermal continuum of Ceres is clearly visible in the late 2012 observations, whereas in the 2013 data it is next to a weaker emission line detected at the 3σ level. The low outflow velocity (0.3–0.7 km s^{-1}) determined from the offset of the absorption line is comparable to the escape velocity of Ceres (about 0.52 km s^{-1}; ref. 18), showing that a fraction of the evaporated water does not escape from Ceres. For line strengths and offset information, see Extended Data Table 3.

The strength of the absorption is variable on short timescales (hours; Fig. 2) as well as on longer timescales (weeks and months; Extended Data Fig. 1 and Extended Data Table 3). We interpret the short-term variation in terms of localized sources on Ceres rotating into and out of the hemisphere visible by Herschel. Figure 2 shows the correlation of the strength of the absorption line with the position of features on the

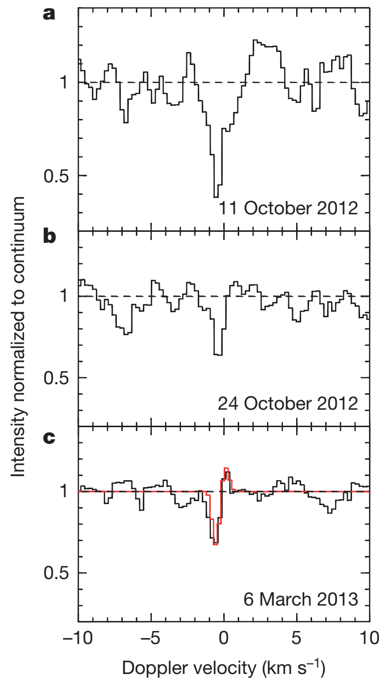

Figure 1 | Submillimetre water absorption line from the dwarf planet (1) Ceres. The spectra of the ground-state transition line 1_{10}–1_{01} of ortho-water at 556.939 GHz were obtained on 11.83–11.92 October 2012 UT (**a**), 24.84–24.96 October 2012 UT (**b**) and 6.13–6.55 March 2013 UT (**c**), with HIFI's Wide-Band Spectrometer. The spectra, which are the averages of the linear H and V polarizations, were divided by the Ceres continuum thermal emission. The abscissa represents the Doppler velocity in the Ceres frame, after correction for the relative motion between Ceres and Herschel. The spectral resolution is 1.1 MHz (0.5 km s^{-1}) with 0.6 MHz sampling. The water line is seen in absorption against the thermal emission of Ceres. Material moving towards the observer causes the absorption line to be blue-shifted. In the 6 March spectrum (**c**), a redshifted emission line is visible next to the blue-shifted absorption line, showing that the exosphere of Ceres extends towards the limbs. The possible polarization of this line is discussed in the Supplementary Information. Overplotted on the 6 March spectrum is a model of the spectrum of the water line for two active spots 60 km in diameter situated on the surface of Ceres (red spectrum in **c**). The simulation takes into account the variation of the sub-observer point longitude during the 10-hour-long observation. The model spectrum is adjusted to the depth of the observed spectrum. The relative strengths of the redshifted and blue-shifted peaks are correctly reproduced.

[1]European Space Agency, European Space Astronomy Centre, PO Box 78, Villanueva de la Cañada 28691, Spain. [2]Laboratoire d'études spatiales et d'instrumentation en astrophysique, Observatoire de Paris, CNRS, Université Pierre et Marie Curie (UPMC), Université Paris-Diderot, 5 Place Jules Janssen, 92195 Meudon, France. [3]Jet Propulsion Laboratory, Pasadena, 4800 Oak Grove Drive, La Cañada Flintridge, California 91011, USA. [4]Institut de Mécanique Céleste et de Calcul des Éphémérides, Observatoire de Paris, Unité Mixte de Recherche (UMR) 8028. CNRS, 77 Avenue Denfert Rochereau, 75014 Paris, France. [5]Max-Planck-Institut für extraterrestrische Physik (MPE), Giessenbachstrasse 1, 85748 Garching, Germany.

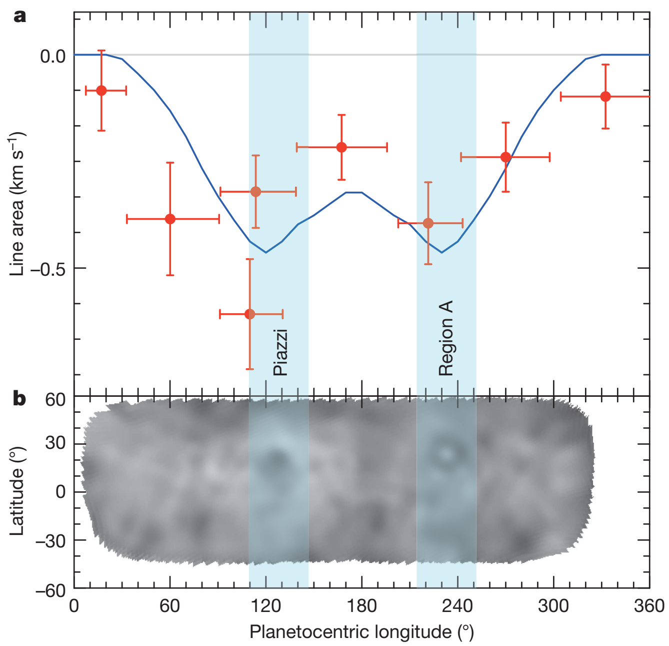

Figure 2 | Variability of water absorption on 6 March 2013. a, Line area of the water absorption line (normalized to the continuum emission of Ceres) at 557 GHz as a function of the longitude of the sub-observer point. Measurements are shown as red dots; error bars on the intensity are 1σ and the horizontal bars show the range of sub-observer longitudes covered by individual measurements. The two conflicting data points at sub-observer point longitude $\Lambda \approx 110^\circ$ were taken within a time interval of 9 hours (corresponding to the rotation period of Ceres), and suggest temporal variability at the regional scale. Vertical bands indicate the planetocentric longitude of the dark regions: Piazzi (longitude, 123°, latitude +21°) and Region A (longitude 231°, latitude +23°)[14,15,19]. The curve in blue is the result of a gas-kinetic model of the exosphere of Ceres[21] (see Supplementary Information). Water is released from localized sources 60 km in diameter situated at the longitudes and latitudes of regions Piazzi and Region A, with a total production rate of 10^{26} molecules per second for each source. The surface temperature of Ceres varies from 235 K (subsolar, that is, when the Sun is at zenith) to 168 K (morning and evening). The excitation and radiative transfer models of the water 1_{10}–1_{01} line include excitation of the vibrational bands by the Sun's infrared radiation, excitation of the rotational lines by thermal radiation from Ceres, collisions with water and self-absorption effects[22] (see Supplementary Information). **b**, A map of Ceres from near-infrared adaptive-optics imaging observations[14]. Piazzi and Region A are seen as dark regions, with a bright centre within Region A.

Ceres surface that are known from ground-based[14,15] and Hubble Space Telescope[19] observations. In all observations that detected water vapour from Ceres, the absorption line strength is strongly correlated with the visibility of surface areas identified as dark regions (about 5% darker than the average surface) in near-infrared observations. We identify those regions as the likely source of most of the evaporating water. A bright region known from observations in the visible region of the spectrum does not appear to contribute. Possibly, the dark regions are warmer than the average surface, resulting in efficient sublimation of small water-ice reservoirs.

Although the small number of observations does not allow a unique interpretation of the long-term variation, the lack of detection of the water line at 2.94 astronomical units (AU; where 1 AU is the mean distance from Earth to the Sun) in November 2011 and its first detection at 2.72 AU are consistent with the steep increase of water-ice sublimation between 3 AU and 2.5 AU (ref. 20). In addition, the larger absorption strength on 11 October 2012 compared to the observations two weeks later and five months later suggests sporadic changes in the water evaporation. Given that the spin axis of Ceres is nearly perpendicular to its orbital plane[14], we expect seasonal variations driven by spin-axis obliquity to contribute little to the variability.

We analysed the water exosphere of Ceres with a gas kinetic Direct Simulation Monte Carlo[21] model (Extended Data Fig. 2) that considers water vapour to be ejected from localized sources, and then to slow down in Ceres' gravity field. To simulate water spectra, we use a state-of-the-art two-dimensional excitation model[22], which considers excitation by radiation from Ceres and the Sun and collisional excitation (see details in Supplementary Information). The temporal variation of the absorption line observed on 6 March 2013 is well described by a model that considers outgassing from two sources coincident with dark regions Piazzi and Region A (Fig. 2). Modelling predicts line emission at positive velocities (Fig. 1), caused by gas expansion from dense to more rarefied regions. The resulting total production rate of about 2×10^{26} molecules (or 6 kg) per second of water requires only a tiny fraction of the Ceres surface to be covered by water ice. The surface of Ceres receives on average a solar input power of approximately 50 W m^{-2} (a quarter of the total solar power at the heliocentric distance of Ceres, with the factor 1/4 being the ratio between the cross-section of Ceres and its surface area). Because Ceres is located in the transition range between the outer Solar System, where most of the solar energy will be re-emitted as thermal radiation, and the inner Solar System, where most of the energy will go into sublimation of the ice, we assume that half of the energy will be used for sublimation. With a latent heat of sublimation of 2.5×10^6 J kg^{-1}, the corresponding sublimation rate is 10^{-5} kg m^{-2} s^{-1}. To sublimate 6 kg s^{-1} of water ice, Ceres must have a surface area covered with water ice of 0.6 km^2, or approximately 10^{-7} of its total surface area. If the activity is restricted to areas with a radius of about 100 km (the approximate size of the identified source regions), the active surface fraction required within those areas is still very small ($<10^{-5}$ of the surface area of the identified source regions).

An unexpected aspect of the data is that the absorption line appears to be strongly linearly polarized in October 2012, whereas no significant polarization was seen in March 2013. See Extended Data Table 3, Extended Data Fig. 3, and Supplementary Information for further analysis.

The measured water production is two orders of magnitudes higher than is predicted from a model of sublimation maintained from water supplied from the interior of Ceres[23]. In addition, the water activity is most probably not concentrated on polar regions, where water ice would be most stable. We propose two mechanisms for maintaining the observed water production on Ceres. The first is cometary-type sublimation of (near) surface ice. In this case the sublimating ice drags near-surface dust with it and in this way locally removes the surface layer and exposes fresh ice. Transport from the interior is not required. The second mechanism is geysers or cryovolcanoes, for which an interior heat source is needed. For Jupiter's satellite Io and Saturn's moon Enceladus the source of activity is dissipation of tidal forces from the planet[24,25]. That can be excluded for Ceres, but some models suggest that a warm layer in the interior heated by long-lived radioisotopes may maintain cryovolcanism on Ceres at the present time (ref. 26 and references therein).

One way of distinguishing between the two mechanisms is to analyse the variation of the water activity of Ceres over its orbit. Taking the activity of main-belt comets as a reference, cometary activity is expected to be concentrated at the perihelion passage[5]. On the other hand, cryovolcanism receives its energy from the interior and so no dependence on heliocentric distance would be seen, although sporadic variations of activity are likely. The currently available data appear to be consistent with the cometary hypothesis, but more observations are needed to distinguish between these possibilities (see Fig. 3).

Although ground- and space-based observations may further map the behaviour of Ceres over its orbit, the Dawn spacecraft mission[27] arriving to orbit Ceres in early 2015 is expected to be key in providing a long-term follow-up on the water outgassing behaviour of Ceres. In particular, it will provide long-term monitoring of the water outgassing concentration and stability of the activity in the dark regions where we suggest that the water-ice mantle of Ceres may reach the surface. Two of the instruments on Dawn—the near-infrared spectrometer (VIR)

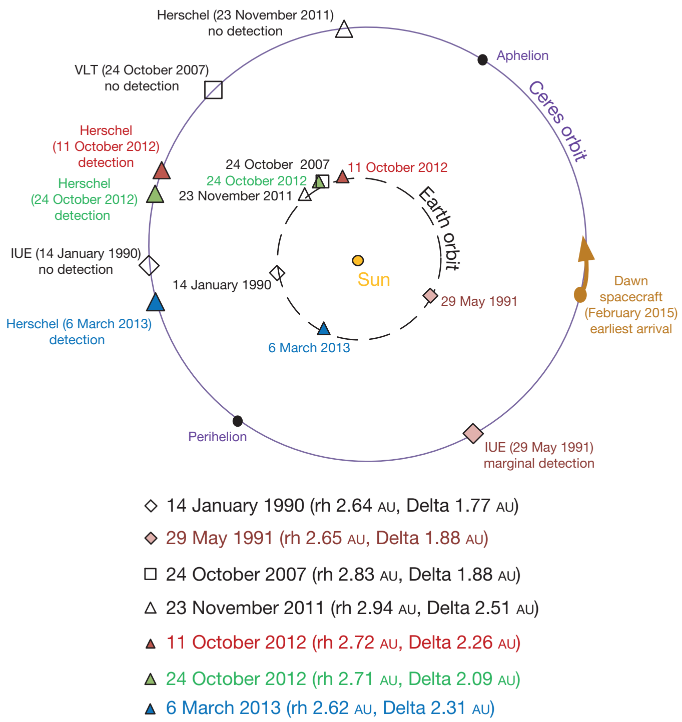

Figure 3 | Water production of Ceres versus position on its orbit. Searches for water activity on Ceres were performed with the International Ultraviolet Explorer (IUE), the Very Large Telescope (VLT), and Herschel. The inner orbit is that of Earth, the outer orbit that of Ceres. rh is the heliocentric distance of Ceres and Delta is the distance between Ceres and the observer. If cometary activity is the source of water on Ceres we would expect the onset of activity to appear well before perihelion before becoming much weaker at some time after perihelion. The pre-perihelion data are consistent with that picture. No activity was detected by VLT and Herschel at less than 2.83 AU; then Herschel detected activity in all observations within 2.72 AU. The non-detection by IUE at almost the same orbital position as one of the Herschel observations three orbital periods earlier can be explained by the higher sensitivity of Herschel for near-equatorial sources. The single observation postperihelion (a marginal detection by IUE) does not allow us to draw conclusions about the behaviour when Ceres is receding from the Sun. Dawn will visit Ceres on the postperihelion arc. The water absorption was strongest in the first Herschel detection on 11 October 2012, well before passing perihelion. To first order this is not what we would expect for cometary activity. It may have been caused by an analogue of a cometary outburst. Alternatively, it could have been a volcanic eruption. In that case, the correlation of the detectability with heliocentric distance may be coincidental. Additional observations are required to distinguish better between different mechanisms for the water activity.

and the gamma ray and neutron detector (GRaND)—may contribute significantly to this task. Although no observations of water are available for the orbital position of Ceres at the time of its arrival (Fig. 3) and the heliocentric distances in the spacecraft's initial few months around Dawn of 2.85–2.95 AU appear to be unfavourable for detecting activity, it may be that the post-perihelion activity is maintained to larger distances.

The identification of more than one water source on Ceres suggests outgassing from a small ice fraction near the surface as opposed to sporadic activity triggered by a singular event like a recent large impact. This supports the idea that Ceres possesses an icy mantle, and it also implies that we have detected water activity in the asteroid main belt. If the water is from cometary sublimation, it demonstrates that activity driven by water sublimation is not limited to classical comets, but is present in the asteroid belt as well. This supports the new vision of our Solar System with a continuum in composition and ice content between asteroid and comet populations[28].

Online Content Any additional Methods, Extended Data display items and Source Data are available in the online version of the paper; references unique to these sections appear only in the online paper.

Received 23 August; accepted 26 November 2013.

1. Walsh, K. J., Morbidelli, A., Raymond, S. N., O'Brien, D. P. & Mandell, A. M. A low mass for Mars from Jupiter's early gas-driven migration. *Nature* **475,** 206–209 (2011).
2. Campins, H. *et al.* Water ice and organics on the surface of the asteroid 24 Themis. *Nature* **464,** 1320–1321 (2010).
3. Rivkin, A. S. & Emery, J. P. Detection of ice and organics on an asteroidal surface. *Nature* **464,** 1322–1323 (2010).
4. Licandro, J. et al. (65) Cybele: detection of small silicate grains, water-ice, and organics. *Astron. Astrophys.* **525,** A34 (2011).
5. Jewitt, D. The active asteroids. *Astron. J.* **143,** 66 (2012).
6. Lebofsky, L. A., Feierberg, M. A., Tokunaga, A. T., Larson, H. P. & Johnson, J. R. The 1.7- to 4.2-micron spectrum of asteroid 1 Ceres: evidence for structural water in clay minerals. *Icarus* **48,** 453–459 (1981).
7. King, T. V. V., Clark, R. N., Calvin, W. M., Sherman, D. M. & Brown, R. H. Evidence for ammonium-bearing minerals on Ceres. *Science* **255,** 1551–1553 (1992).
8. Milliken, R. E. & Rivkin, A. S. Brucite and carbonate assemblages from altered olivine-rich materials on Ceres. *Nature Geosci.* **2,** 258–261 (2009).
9. Thomas, P. C. *et al.* Differentiation of the asteroid Ceres as revealed by its shape. *Nature* **437,** 224–226 (2005).
10. McCord, T. B. & Sotin, C. Ceres: evolution and current state. *J. Geophys. Res.* **110,** E05009 (2005).
11. Castillo-Rogez, J. C. & McCord, T. B. Ceres' evolution and present state constrained by shape data. *Icarus* **205,** 443–459 (2010).
12. A'Hearn, M. F. & Feldman, P. D. Water vaporization on Ceres. *Icarus* **98,** 54–60 (1992).
13. Rousselot, P. *et al.* A search for water vaporization on Ceres. *Astron. J.* **142,** 125 (2011).
14. Carry, B. *et al.* Near-infrared mapping and physical properties of the dwarf-planet Ceres. *Astron. Astrophys.* **478,** 235–244 (2008).
15. Carry, B. *et al.* The remarkable surface homogeneity of the Dawn mission target (1) Ceres. *Icarus* **217,** 20–26 (2012).
16. de Graauw, Th *et al.* The Herschel-Heterodyne Instrument for the Far-Infrared (HIFI). *Astron. Astrophys.* **518,** L6 (2010).
17. Pilbratt, G. L. *et al.* Herschel Space Observatory. An ESA facility for far-infrared and submillimetre astronomy. *Astron. Astrophys.* **518,** L1 (2010).
18. Carry, B. Density of asteroids. *Planet. Space Sci.* **73,** 98–118 (2012).
19. Li, J.-Y. *et al.* Photometric analysis of 1 Ceres and surface mapping from HST observations. *Icarus* **182,** 143–160 (2006).
20. Biver, N. *et al.* The 1995–2002 long-term monitoring of comet C/1995 O1 (Hale–Bopp) at radio wavelength. *Earth Moon Planets* **90,** 5–14 (2002).
21. Crifo, J. F., Loukianov, G. A., Rodionov, A. V. & Zakharov, V. V. Comparison between Navier–Stokes and direct Monte-Carlo simulations of the circumnuclear coma I. Homogeneous, spherical sources. *Icarus* **156,** 249–268 (2002).
22. Zakharov, V., Bockelée-Morvan, D., Biver, N., Crovisier, J. & Lecacheux, A. Radiative transfer simulation of water rotational excitation in comets. Comparison of the Monte Carlo and escape probability methods. *Astron. Astrophys.* **473,** 303–310 (2007).
23. Fanale, F. P. & Salvail, J. R. The water regime of asteroid (1) Ceres. *Icarus* **82,** 97–110 (1989).
24. Peale, S. J., Cassen, P. & Reynolds, R. T. Melting of Io by tidal dissipation. *Science* **203,** 892–894 (1979).
25. Howett, C. J. A., Spencer, J. R., Pearl, J. & Segura, M. High heat flow from Enceladus' south polar region measured using 10–600 cm-1 Cassini/CIRS data. *J. Geophys. Res.* **116,** E03003 (2011).
26. McCord, T. B., Castillo-Rogez, J. & Rivkin, A. Ceres: its origin, evolution and structure and *Dawn's* potential contribution. *Space Sci. Rev.* **163,** 63–76 (2011).
27. Russell, C. T. & Raymond, C. A. The Dawn mission to Vesta and Ceres. *Space Sci. Rev.* **163,** 3–23 (2011).
28. Gounelle, M. *et al.* in *The Solar System Beyond Neptune* (eds Barucci, M. A., Boehnhardt, H., Cruikshank, D. P. & Morbidelli, A.) 525–541 (Univ. Arizona Press, 2008).

Supplementary Information is available in the online version of the paper.

Acknowledgements Herschel is an ESA space observatory with science instruments provided by European-led principal investigator consortia and with important participation by NASA. The HIFI was designed and built by a consortium of institutes and university departments from across Europe, Canada and the United States under the leadership of SRON, the Netherlands Institute for Space Research, and with major contributions from Germany, France and the USA. This development was supported by national funding agencies: CEA, CNES, CNRS (France); ASI (Italy); and DLR (Germany). Additional funding support for some instrument activities was provided by the ESA. We thank the team at the Herschel Science Centre for their flexibility in scheduling the observations. We thank the Herschel Project Scientist and the Time Allocation Committee for the allocation of Director Discretionary Time. B.C. acknowledges support from the faculty of the European Space Astronomy Centre (ESAC). We thank A. Pollock for proofreading the final text.

Author Contributions M.K. proposed the observations of Ceres with HIFI as part of L.O'R.'s MACH-11 Guaranteed Time Program. M.K., L.O'R., D.B.-M., B.C., D.T. and A.M. planned the observations. M.K., D.B.-M., B.C., D.T., R.M. and J.C. contributed to the data analysis. The modelling was performed by D.B.-M., V.Z., S.L., P.v.A. and T.M. The manuscript was written by M.K., L.O'R., D.B.-M., B.C. and M.A.B. All authors discussed the results and reviewed the manuscript.

Author Information Reprints and permissions information is available at www.nature.com/reprints. The authors declare no competing financial interests. Readers are welcome to comment on the online version of the paper. Correspondence and requests for materials should be addressed to M.K. (michael.kueppers@sciops.esa.int).

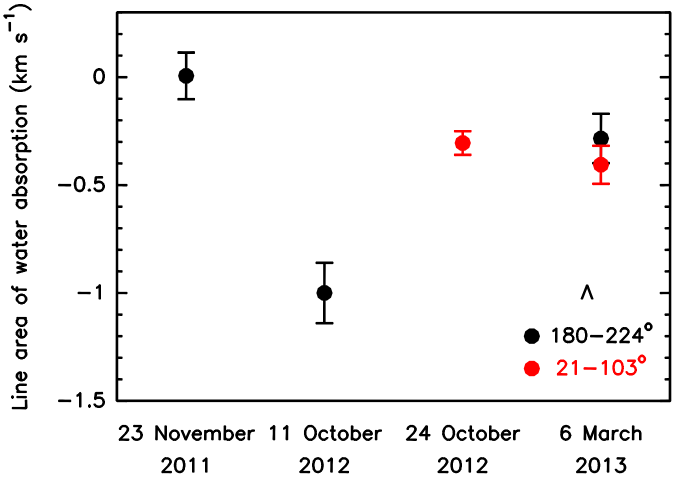

Extended Data Figure 1 | Long-term variability of water absorption. The absolute value of the area of the water absorption line at 557 GHz (line area normalized to Ceres continuum emission) is plotted for dates of observations covering the same sub-observer point longitudes: $\Lambda = 180^\circ$–204° on 23 November 2011, 11 October 2012 and 6 March 2013 (black dots); $\Lambda = 21^\circ$–103° on 24 October 2012 and 6 March 2013 (red dots). Error bars are 1σ. The strength of the absorption is variable on timescales of hours or months.

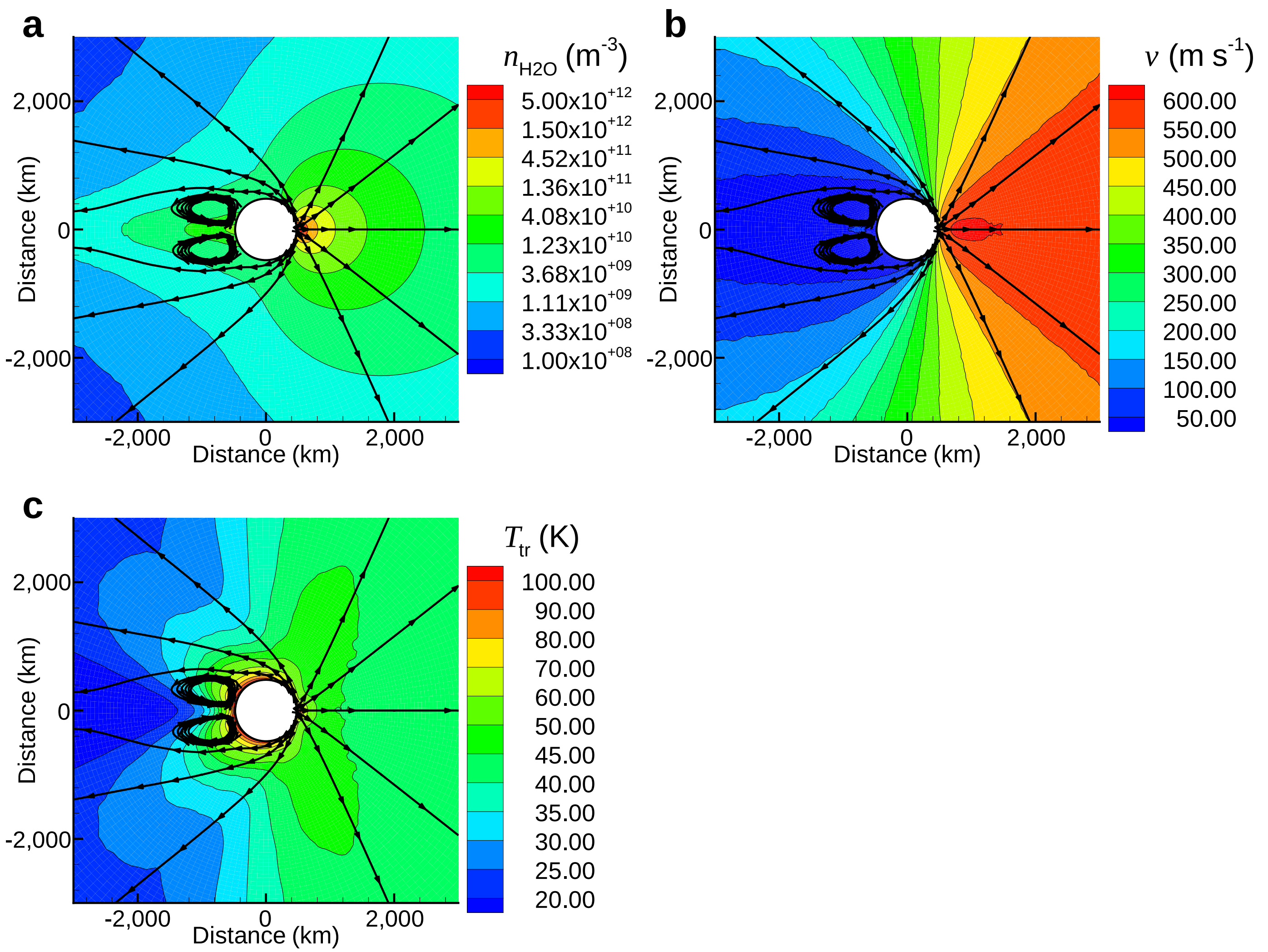

Extended Data Figure 2 | Direct Simulation Monte Carlo calculations of the exosphere of Ceres. a–c, Number density n_{H2O} (**a**), velocity v (**b**) and translational temperature T_{tr} (**c**) for water outgassing from an active spot about 60 km in diameter situated on the surface of Ceres at the subsolar point. The Sun is towards the right. The total water production rate is 10^{26} molecules per second. The Ceres surface temperature varies from 235 K (subsolar) to 168 K. See Supplementary Information. Stream lines are shown in black. The vortex seen on the night side is caused by the competition of molecules falling back on the surface owing to gravity and those molecules diffusing outwards. The local maximum in velocity observed above the active spot is also an effect of gravity. The gravity of Ceres causes 3% of the evaporated molecules to fall back to the surface, whereas 7% fall back owing to collisions between water molecules in the atmosphere.

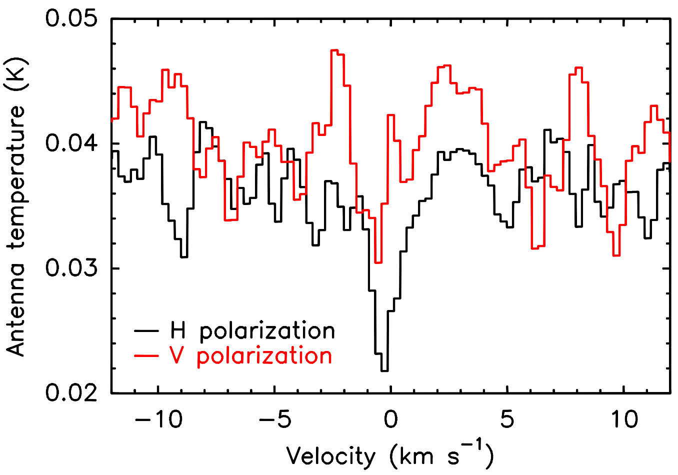

Extended Data Figure 3 | The spectrum from 11 October 2012 in H and V polarizations. Although there is no significant polarization in the continuum, the line area is about 2.5 times larger in horizontal polarization than in the marginal detection of the line in vertical polarization.

Extended Data Table 1 | Overview of the acquired data

Start date and time	Duration	r	Δ	Sub-observer point		Sub-solar point		Phase
				Λ	ε	Λ_S	ε_S	ϕ
(UT)	(s)	(AU)	(AU)	(°)	(°)	(°)	(°)	(°)
2011-11-23 11:31:20	4010	2.94	2.51	224-180	5	243-200	3	19
2012-10-11 19:53:46	8245	2.72	2.26	247-156	1	227-139	−1	21
2012-10-24 20:04:28	8575	2.71	2.09	103-8	1	84-350	−1	19
2013-03-06 03:05:42	8575	2.62	2.31	130-35	−7	152-57	−3	22
2013-03-06 05:30:03	9146	2.62	2.31	34-293	−7	56-318	−3	22
2013-03-06 08:03:55	9146	2.62	2.31	292-192	−7	317-214	−3	22
2013-03-06 10:37:47	9146	2.62	2.31	191-90	−7	213-111	−3	22

Geometric parameters of the observations are the heliocentric distance of Ceres r, the Ceres–Herschel distance Δ, the sub-observer point longitude Λ and subsolar point longitude Λ_S at the beginning and end of each observation[14,29], the sub-observer point latitude ε and subsolar point latitude ε_S (refs 14 and 29), and the phase angle ϕ. The Herschel observation identification numbers (Obsids) are 1342232694 (23 November 2011), 1342253122 (11 October 2012), 1342254428 (24 October 2012) and 1342266018–1342266021 (6 March 2013).

29. Chamberlain, M. A., Sykes, M. V. & Esquerdo, G. A. Ceres light curve analysis—period determination. *Icarus* **188,** 451–456 (2007).

Extended Data Table 2 | Continuum brightness in the spectra

Date (UT)		Measured continuum (Jy)	Expected continuum (Jy)
23.48-23.53	November 2011	7.24 ± 0.65	7.35 ± 0.4
11.83-11.92	October 2012	8.71 ± 1.16	9.78 ± 0.5
24.84-24.96	October 2012	11.48 ± 0.72	11.54 ± 0.6
6.13-6.55	March 2013	8.61 ± 0.62	8.74 ± 0.4

Measured and expected brightness of the continuum. The expected thermal continuum was calculated with a thermophysical model[30]. The estimated accuracy of the model is 5%.

30. Müller, T. G. *et al.* Herschel celestial calibration sources: four large main-belt asteroids as prime flux calibrators for the far-IR/sub-mm range. *Exp. Astron.* http://dx.doi.org/10.1007/s10686-013-9357-y (in the press).

Extended Data Table 3 | Characteristics of H_2O spectra

Date (UT)		Polarization	Line area (km s^{-1})	Offset (km s^{-1})	Width (km s^{-1})	Absorbance (%)
23.48-23.53	November 2011	H+V	0.07± 0.10	-	-	< 10
11.83-11.92	October 2012	H	−1.07 ± 0.12	−0.26 ± 0.07	1.37 ± 0.21	74
		V	−0.43 ± 0.12	−0.76 ± 0.15	0.96 ± 0.26	42
		H+V	−0.79 ± 0.10	−0.40 ± 0.09	1.43 ± 0.22	52
24.84-24.96	October 2012	H	−0.56 ± 0.09	−0.72 ± 0.11	1.21 ± 0.19	44
		V	−0.22 ± 0.06	−0.16 ± 0.09	0.61 ± 0.18	34
		H+V	−0.31 ± 0.06	−0.39 ± 0.07	0.73 ± 0.16	39
6.13-6.55	March 2013	H	−0.27 ± 0.04	−0.67 ± 0.05	0.69 ± 0.10	37
		V	−0.20 ± 0.04	−0.69 ± 0.09	0.67 ± 0.18	28
		H+V	−0.24 ± 0.03	−0.68 ± 0.05	0.68 ± 0.09	33

Results of Gaussian fits to the water 1_{10}–1_{01} absorption line, after normalizing by the thermal continuum emission from Ceres. Offset refers to the radial velocity of the line centre relative to that of Ceres. The last column provides the absorbance (the percentage of the continuum that is absorbed) at the line centre from a Gaussian fit to the absorption line (1σ upper limit for the first observation). The V/H line area ratios are 0.40 ± 0.12, 0.38 ± 0.13 and 0.74 ± 0.20, for 11 October, 24 October and 6 March, respectively.